A chemical imidization method to avoid pore collapsing and selective layer thickening of PMDA-ODA polyimide nanofiltration membranes

Rui Zhang, Jingjing Xue, Yuan Li, Bing Cao*, Pei Li*

College of Materials Science and Engineering, Beijing University of Chemical Technology, Chaoyang District North Third Ring Road 15, Beijing 100029, China, email: zhangrui1@mail.buct.edu.cn (R. Zhang), 18703641@qq.com (J. Xue), zr10000@sina.com (Y. Li), bcao@mail.buct.edu.cn (B. Cao), lipei@mail.buct.edu.cn (P. Li)

ABSTRACT

To suppress pore collapsing and selective layer thickening of Poly (pyromellitic dianhydride-co-4,4′-oxydianiline) (PMDA-ODA) nanofiltration (NF) membrane during imidization, we proposed a novel two step method. Specifically, a PMDA-ODA polyamic acid (PAA) polymer dope was cast on top of a non-woven polyester fabric and then underwent non-solvent induced phase inversion to form a PMDA-ODA PAA membrane. The membrane was subsequently dried by solvent exchange and chemically imidized to form PMDA-ODA PI membrane. Compared with the thermally imidized PMDA-ODA PI membrane, which had a thick selective layer of 14.5 µm and pure water permeability of 1.5 L/(m²·h·bar), membrane fabricated using the new method had a thinner selective layer of 1.04 µm and 7 times higher pure water permeability of 10.4 L/(m²·h·bar) without losing rejections. Other than that, the NF membrane also showed good separation properties in organic solvent systems. It showed rejections of 87%~95% to Rose Bengal in DMF, THF, and DMSO, with stable permeabilities of 6.1–8.0 L/(m²·h·bar), at a trans-membrane pressure of 20 bar for at least 24 h. Therefore, the PMDA-ODA PI membranes had great potential for NF in both water and organic solvent systems.

Keywords: PMDA-ODA polyimide; Nanofiltration; Chemical imidization; Non-woven substrate; Flat sheet composite membrane

1. Introduction

NF membranes have pore sizes in a range from sub-nano to a few nanometers and have been mainly applied in separation to aqueous systems such as desalination or wastewater reclamation [1,2]. However, most of the industrial processes utilize organic solvents. Separating or purifying products from organic solvents are energy intensive by using distillation or extraction technologies [3]. Organic solvent nanofiltration (OSN) significantly reduce energy consumption of the above mentioned processes due to avoidance of phase change in distillation and solvent regeneration in extraction [4]. Therefore, in the last two decades, OSN membranes have been extensively studied and applied in various areas such as solvent recovery [5–7], edible oil processing enrichment [8,9], purification of bio-active compounds [10,11], isolation and concentration of pharmaceuticals [12,13], and so forth.

Inorganic materials such as Al_2O_3, ZrO_2, TiO_2, or SiO_2 are stable in a wide temperature range, and inert to most organic solvents [14,15]. Membranes made of these materials have been successfully applied in OSN processes [16–18]. However, inorganic membranes are typically expensive and encounter problems such as difficult processing and brittleness. Their commercial applications are still limited. By contrast, polymeric OSN membranes are low cost, high flexible and relatively ease for manufacture. At present, commercial polymeric OSN membranes such as STARMEM (W.R.GRACE), MPF (KOCH), Desal-DK (OSMONICS), DuraMem (EVONIK), dominate the OSN market [19–21]. STARMEM and Desal-DK membrane are made of polyimide (PI); MPF and DuraMem membranes use polydimethylsiloxane (PDMS) as the separating layer material. Other than these polymers, polyacrylonitrile (PAN) [22–24], poly-

---

*Corresponding author.

etherimide (PEI) [25], polybenzimidazole (PBI) [26], poly-amide-imide (PAI), poly (ether ether ketone) (PEEK) [26], polydopamine [26], polymers of intrinsic microporosity (including PTMSP, PMP and PIM-1) [27], and polydicyclo-pentadiene [28] have also been reported for making OSN membranes. Among these materials, PI such as Matrim-id™ 5218 and Lenzing P84 [29–31], and PAI such as Torlon are extensively studied because of their excellent thermal mechanical properties, good chemical stabilities and com-mercial availability. However, because they are soluble in many polar aprotic solvents such as N-methyl-2-pyr-rolidone (NMP), dimethylacetamide (DMAc), dimeth-ylformamide (DMF) etc., crosslinking treatments, which may decrease the membrane flux, has to be performed to increase their solvent resistances [32,33].

In our opinion, NF membranes having good separation properties in both water and organic solvent systems shall be more applicable for industrial applications. The key is to utilize materials with excellent solvent resistance, high mechanical strength and ability of maintaining these prop-erties at required working conditions. PMDA-ODA poly-imide (chemical structure shown in Fig. 1) has high glass transition temperature (T_g, 368.1°C), excellent solvent resis-tance, and is commercial available with low cost. However, due to the insolubility of PMDA-ODA, membranes have to be fabricated using its intermediate polymer-poly (amic acid), which is soluble in many polar organic solvents, through a non-solvent induced phase inversion method, and the nascent poly(amic acid) membranes are imidized to form PI membranes.

In our previous works, PMDA-ODA NF membranes were prepared using a thermal imidization method [34,35]. The membranes had high dye rejections (>92%), excellent solvent resistance but low permeabilities of 0.8~1.0 L/(m²·h·bar) which was caused by two reasons. First, nascent PAA membranes were vacuum dried of which the pores tended to collapse due to the high surface tension of water (72.5 dyn/cm at 20°C). Second, imidization of dry PAA membranes was carried out at 300°C which was much higher than T_g of PMDA-ODA PAA (107°C [36]) so that membrane porous structure might collapse because of the existence of residual stress.

In this study, to mitigate pore collapsing in the mem-brane drying process, solvent-exchange protocol was uti-lized. Specifically, water-wet membrane was soaked in isopropanol and then in n-hexane before dried in air. The much lower surface tension of n-hexane (18.4 dyn/cm at 20°C) would limit pore shrinkages during drying. To void high imidization temperature, PAA membranes were chem-ically imidized at a much lower temperature of 100°C. In addition, to further reduce shrinkage of PAA membrane in the chemical imidization process, polyester non-woven fabrics with different pore sizes were used as supporting

layer for PMDA-ODA NF membranes. We expected that this method would at least alleviate shrinkage at membrane horizontal directions due to support of the non-woven fab-ric. Effects of non-woven fabrics, chemical imidization to morphologies and separation performance of the PMDA-ODA NF membranes were studied systematically by com-paring these properties to membranes prepared by thermal imidization in both water and organic solvent systems. At last, the solvent resistance was evaluated by applying the PMDA-ODA NF membranes to separate dyes in varied strong polar aprotic organic solvents.

2. Experiments

2.1. Materials:

15 wt.% PMDA-ODA PAA/N-methyl-2-pyrrolidone (NMP) dope was purchased from Changzhou Sunchem High Performance Polymer Co., Ltd. (Changzhou, China) and stored in a refrigerator before use. Acetic anhydride (Ac₂O) and triethylamine (TEA) were purchased from Sino-pharm Chemical Reagent Beijing Co., Ltd. (Beijing, China). Two polyester non-woven fabrics branded as TER-80 and UAF-48 were bought from Shanghai Jiujun Filter Media Co. Ltd. (Shanghai, China). Isopropanol, n-hexane, ethanol, ethyl acetate, dimethylacetamide (DMAc), tetrahydrofuran (THF), dimethylformamide (DMF), and glycerol were got from Aladdin Co., Ltd. (China). Hydrochloride acid (37.5 wt.%), and sodium hydroxide were purchased from Tianjin Fu Chen Chemical Reagents Factory (Tianjin, China). Dyes including Congo Red, Rose Bengal, Fast Green FCF, and Rhodamine B were got from J&K Scientific Co. Ltd. (China). All chemicals were used as received without further puri-fication.

2.2. Fabrication of PMDA-ODA NF membranes

2.2.1. Thermal imidization

A thermal imidization method reported in our previ-ous research [34] was adopted to fabricate the freestand-ing PMDA-ODA NF membranes. As shown in Fig. 2, in the first step, a 15 wt.% PMDA-ODA PAA polymer dope was cast on a clean glass board using a doctor blade to control a film thickness of 150 μm. The nascent film was immediately immersed in deionized water at room tem-perature for 60 min for phase inversion. In the second step, the water-wet PAA membrane was vacuum dried for 8 h at room temperature. Then, the dry PAA membrane was heated in vacuum to induce imidization [34]. Specifically, the PAA membrane was heated at a rate of 5°C/min, and hold at 200°C for 2.5 h, 250°C for 2 h, and 300°C for 2.5 h, respectively. The resulting PMDA-ODA PI membranes were coded as PI-0.

2.2.2. Chemical imidization

In the chemical imidization process, a freestanding PMDA-ODA PAA membrane was prepared using the same method as described above. The water-wet PAA membrane was subsequently immersed in isopropanol and then in
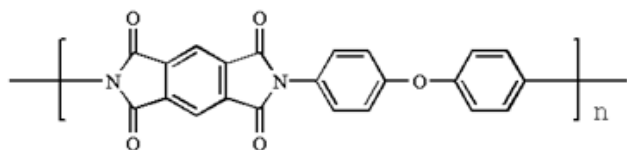
Fig. 1. Chemical structure of PMDA-ODA polyimide.
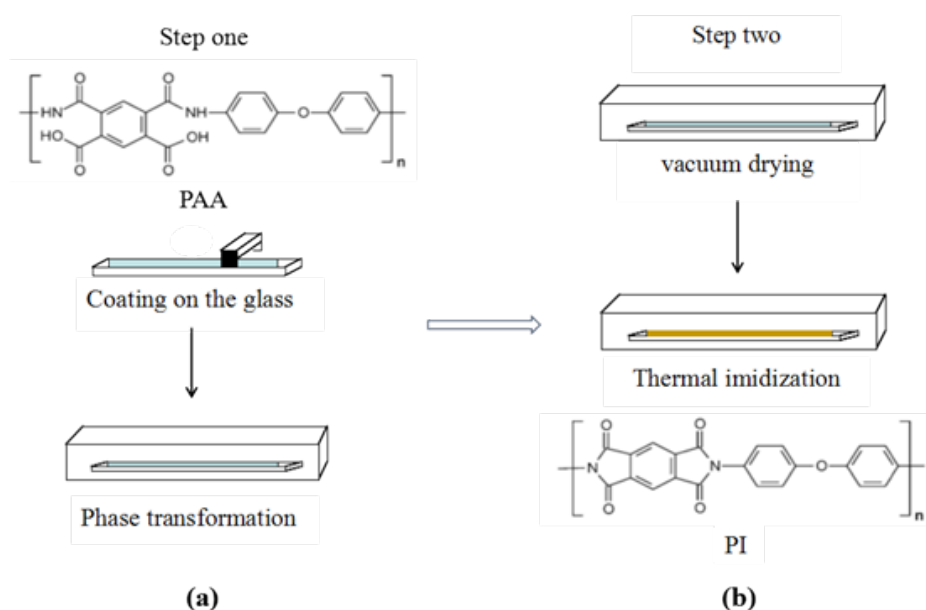
Fig. 2. A schematic diagram of preparing freestanding PMDA-ODA NF membranes using a two-step thermal imidization method: (a) preparing PMDA-ODA PAA membranes via non-solvent induced phase inversion; and (b) fabricating PMDA-ODA membranes by thermal imidization.

n-hexane. The *n*-hexane-wet membrane was chemically imidized through a similar process reported by Li et. al [37]. Specifically, the PAA membrane was immersed in a mixture of acetic anhydride (Ac$_2$O) and triethylamine (TEA) at a volume ratio of 4:1 and heated at 100°C for 36 h for the accomplishment of imidization. The resulting freestanding PMDA-ODA membrane denoted as PI-1 was stored in iso-propanol.

2.2.3. Fabrication of non-woven supported membrane

Two polyester non-woven fabrics, TER-80 and UAF-48, with average pore sizes of 7.07 μm and 25 μm were used as the substrates for preparing PMDA-ODA NF membranes denoted as PI-2 and PI-3, respectively. The non-woven supported NF membranes were also prepared using the two step chemical imidization method except that PMDA-ODA polymer dope was cast on non-woven fabrics instead of glass boards.

2.3. Characterization

2.3.1. ATR-FTIR

An ATR-FTIR spectrometer (Spectrum RX I) purchased from Perkin Elmer (USA) was used to confirm imidization of the PAA membranes. A piece of dry PMDA-ODA PAA membrane or PMDA-ODA PI membrane was placed on a sample holder and the sample surface was scanned by ATR-FTIR in a wavenumber range from 400 to 4000 cm^{-1}.

2.3.2. SEM

Membrane morphologies including upper surface and cross-section were observed using a Hitachi 4700 scanning electron microscope. To obtain a smooth surface, a membrane sample was immersed in liquid nitrogen before fractured. Then, the sample was sputtering coated with gold or palladium ahead of test.

2.3.3. AFM

Three-dimensional surface morphology and membrane roughness were characterized by an Agilent 5500 atomic force microscope. Membrane samples were freeze-dried before test.

2.3.4. TGA

Thermal stabilities of the membranes were tested by Q50 Thermogravimetric Analysis (TGA). Samples were heated from 30°C to 800°C with a heating rate of 10°C/min under N$_2$ atmosphere.

2.3.5. Membrane porosity measurement

To determine membrane porosity, a membrane sample with known length and width was first immersed in iso-propanol for 2 h. After that, the sample was taken out and residual isopropanol on the sample surface was wiped off. Then, weight and thickness were measured and recorded. Finally, the sample was dried and weighed again. Membrane porosity was estimated using Eq. (1):

$$P = \frac{(W_1 - W_2)}{\rho V} \tag{1}$$

where P is sample porosity; W_1 is weight of isopropanol-wet sample; W_2 is weight of dried sample; ρ is density of isopropanol at testing temperature; and V is sample volume.

To determine porosity of the non-woven supported membrane, porosities of the non-woven fabrics (P_n), thickness of the membrane on top of the non-woven (L_1), thicknesses of the non-woven support (L_2), and weights of the wet (W_1) and dry (W_2) non-woven supported membranes were determined. Then, porosity of the membrane (P_m) on top of non-woven support was obtained using Eq. (2):

$$P_m = \frac{(W_1 - W_2 - \rho \times P_n \times V_2)}{(\rho \times P_n \times V_2)} \cdot \frac{L_2}{L_1} \cdot P_n \qquad (2)$$

where V_2 is volume of the non-woven substrate and is estimated using Eq. (3):

$$V_2 = A \times B \times L_2 \qquad (3)$$

where A and B are length and width of the membrane sample, respectively.

2.3.6. Evaluation of solvent resistance of the PMDA-ODA PI membranes

To determine solvent resistance of membranes, the chemically imidized freestanding PI membranes were immersed in varied solvents including ethanol, ethyl acetate, n-hexane, DMF, THF, DMSO, NMP, HCl (pH=1), and NaOH pH=10) for 7 days at room temperature. Weights of the membranes were measured before and after immersion. The weight changes were used to evaluate the solvent resistance of the membranes.

2.3.7. Nanofiltration measurements

Permeabilities and rejections of all PMDA-ODA NF membranes were tested using a stainless steel cross-flow device. A membrane was placed on top of a porous stainless steel disc with an effective filtration area of 16 cm². All experiments were carried out at 30°C. A dye solution with a concentration of 100 mg·L⁻¹ was used as the feed which was circulated and strongly stirred in a feed chamber to minimize the concentration polarization. Permeabilities (J) was determined by directly measuring volume of the permeate using Eq. (4):

$$J = \frac{Q}{S \times t \times P} \qquad (4)$$

where Q is total volume of the permeate (L); S is effective membrane area (m²); t is time to collect the permeate (h); and P is transmembrane pressure (bar). In a typical NF experiment, the system was first running for at least 30 min at a predetermined condition and then permeate was collected to ensure a stable performance. Rejection (R) to dyes was determined by measuring concentrations of permeate and feed solutions using a UV-visible spectrophotometer (TU-1810, China). The maximum absorption wavelength of Rose Bengal is 546–550 nm in UV spectrophotometer. Dye rejection of the membrane was calculated using Eq. (5):

$$R = \left[1 - \frac{C_p}{C_f}\right] \times 100\% \qquad (5)$$

where C_p (mg·L⁻¹) and C_f (mg·L⁻¹) are dye concentrations in the permeate and feed, respectively. At each testing condition, the experiment was repeated for 5 groups of parallel experiments and the average values were reported.

3. Results and discussion

3.1. Conformation of imidization of the PMDA-ODA PI membranes

ATR-FTIR spectra were measured to determine the conversion of imidization reactions of all PMDA-ODA PI membranes. Fig. 3 shows that the PAA membrane exhibits two characteristic peaks at 1550 cm⁻¹ and 1660 cm⁻¹ representing the stretch vibration of the C=O and C-N bands of the acid-amide group. After thermal or chemical imidization, these two peaks disappeared. And three new peaks at 1778 cm⁻¹, 1722 cm⁻¹, and 1378 cm⁻¹ are observed which represent the symmetric stretch vibration, asymmetric stretch vibration of the C=O band and stretch vibration of the C-N-C band in the imide group [34]. Therefore, the disappearance of acid-amide group and the appearance of imide group indicate that PMDA-ODA PAA transforms to polyimide completely after both the thermally and chemically imidized processes.

3.2. Solvent resistance

The weight change% is defined as $(w_0 - w_s)/w_0\%$, where w_0 is sample weight before immersion and w_s is sample weight after immersion.

As listed in Table 1, after imidization, the PI membranes are very stable in all organic solvents including strong polar aprotic solvents such as THF, DMF and DMSO, but are slightly soluble in NMP. In addition, significant weight losses of the PMDA-ODA PI membranes are observed in both acid and alkaline solutions due to the hydrolysis reaction of the imide group [37]. In this case, the PMDA-ODA PI membranes will lose their integrities and high rejection rates. Therefore, the solubility test indicates that the PMDA-ODA PI NF membranes can be applied in most organic solvent systems.

3.3. Thermal stability

Fig. 4 shows that thermal degradation temperatures of freestanding PI-0 and PI-1 membranes are 500°C. While those of the PI-2, PI-3, and pristine non-woven fabric are 380°C. Therefore, the PMDA-ODA PI membranes have better thermal stabilities than the non-woven fabric. Nevertheless, the non-woven supported PI membranes still show good enough thermal stability for the NF applications.

3.4. Membrane morphology

Figs. 5–7 show cross-sections and surface morphologies of the PMDA-ODA PAA membranes and the PMDA-ODA PI membranes. According to Fig. 5, the PMDA-ODA layer thicknesses decrease from 60 μm to 50 μm, 60 μm to 52 μm, 55 μm to 40 μm, and 43 μm to 38 μm, respectively, corresponding PI-0, PI-1, PI-2, and PI-3 membranes, respectively. Reduction rates of the PMDA-ODA layer thickness
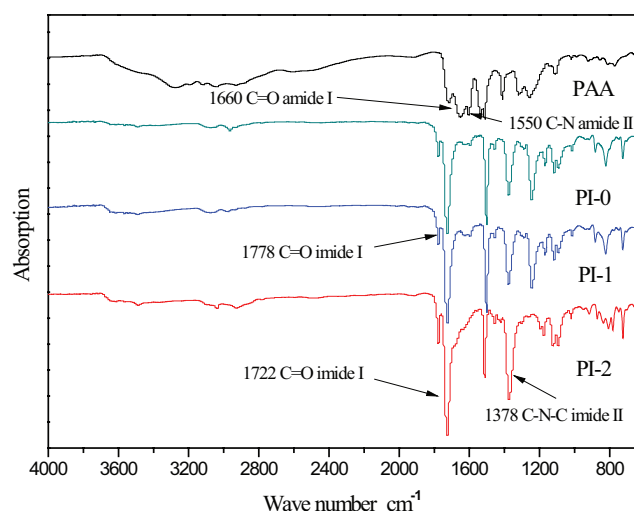
Fig. 3. ATR-FTIR spectra of the PMDA-ODA membranes before imidization (PAA), after thermal imidization (PI-0), chemical imidization (PI-1), and chemical imidization on the membrane with a non-woven support (PI-2).

Table 1
The weight change% of the PMDA-ODA PI membranes after immersion in different solvents for 7 d (standard deviation between±0.2%)

Solvent	Weight change (%)
Ethanol	1.37
Ethyl acetate	1.82
n-hexane	1.42
THF	1.25
DMF	1.76
DMSO	1.08
NMP	3.52
HCl (pH=1)	8.03
NaOH (pH=10)	24.1
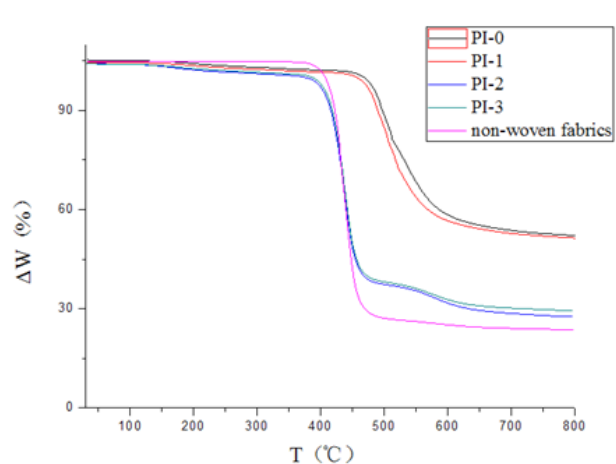
Fig. 4. TGA curves for PI-0, PI-1, PI-2, PI-3 membranes and non-woven fabrics.

are 16.7%, 13.3%, 27.3%, and 11.6%, respectively. Compared with the freestanding membranes, the TER-80 supported membrane shows more reduction percentage. It is different from our expectation that the non-woven support shall alleviate the membrane shrinkage during imidization. However, we observe the formation of wrinkles of the freestanding PI membranes which causes increment in thickness as shown in Fig. 8b. Since the non-woven support prevents the shrinkage on the horizontal directions of the PMDA-DOA layer during imidization, the resulting PI membrane has a flat surface as shown in Fig. 8c. Without formation of wrinkles, PI-2 is thinner than PI-0 and PI-1. The UAF-48 supported membrane has the lowest reduction rate of the PMDA-ODA layer although it also has a flat surface after imidization. This result is attributed to infiltration of PAA polymer dope into the UAF-48 non-woven fabric since it has a very large pore size of 25 μm. Note that, thickness of the PMDA-ODA PAA layer of the PI-3 is 43 μm that is much lower than other PAA membranes. A thinner PMDA-ODA PAA layer may be the reason that reduction in thickness of the PMDA-ODA layer of PI-3 is less obvious.

Fig. 6 shows that the selective layer thicknesses of all the PMDA-ODA PAA membranes are similar (0.61~0.87 μm). This is a reasonable result since all membranes are prepared using polymer dopes with the same PAA concentration and a similar phase-inversion process. A slightly decreased selective layer thickness is observed when the PAA polymer dope is cast on top of the non-woven fabric. The thickness continuously decreases when pore size of the non-woven fabric is bigger. As shown in Figs. 7 a_2, a_3, some dark spots and defects are observed. It indicates that part of the PAA polymer dope solution infiltrates into the non-woven supports. This may cause further decreases in the selective layers' thicknesses of the PAA membranes. However, infiltration of the dope solution does not lead to significant differences in the selective layer thicknesses of the PAA membranes.

Figs. 6 b_0–b_3 show selective layers' thicknesses of the PMDA-ODA PI membranes. Selective layer thickness of PI-0 increases 16.7 times (from 0.87 μm to 14.5 μm) after thermal imidization. Clearly, the high temperature of thermal imidization causes thickening of the selective layer. In contrast, after chemical imidization, selective layer thickness only increases 9.3 times (from 0.86 μm to 8.0 μm). Effects of heat treatment to membrane morphology and performance have been studied extensively [38–40]. It is found that membrane permeability can be greatly preserved if heating temperature is lower than T_g of the membrane material. In this case, the membrane material is still rigid so that the porous structure is maintained. In this study, chemical imidization is performed by soaking the membrane in a AA/TEA mixed solvent and heating at 100°C for 36 h. The sub-T_g imidization method slows down the thickening of the selective layer to some extent. However, since PMDA-ODA PAA is soluble in many organic solvents, it is very likely that during chemical imidization the PAA membranes are plasticized by the AA/TEA mixed solvent. As the membrane material became soft, micropores within the membrane would collapse in presence of the interfacial stresses between the PAA polymer and solvents. Therefore, a 9.3 times increase in the selective layer thickness of the PI-1 membrane is observed.
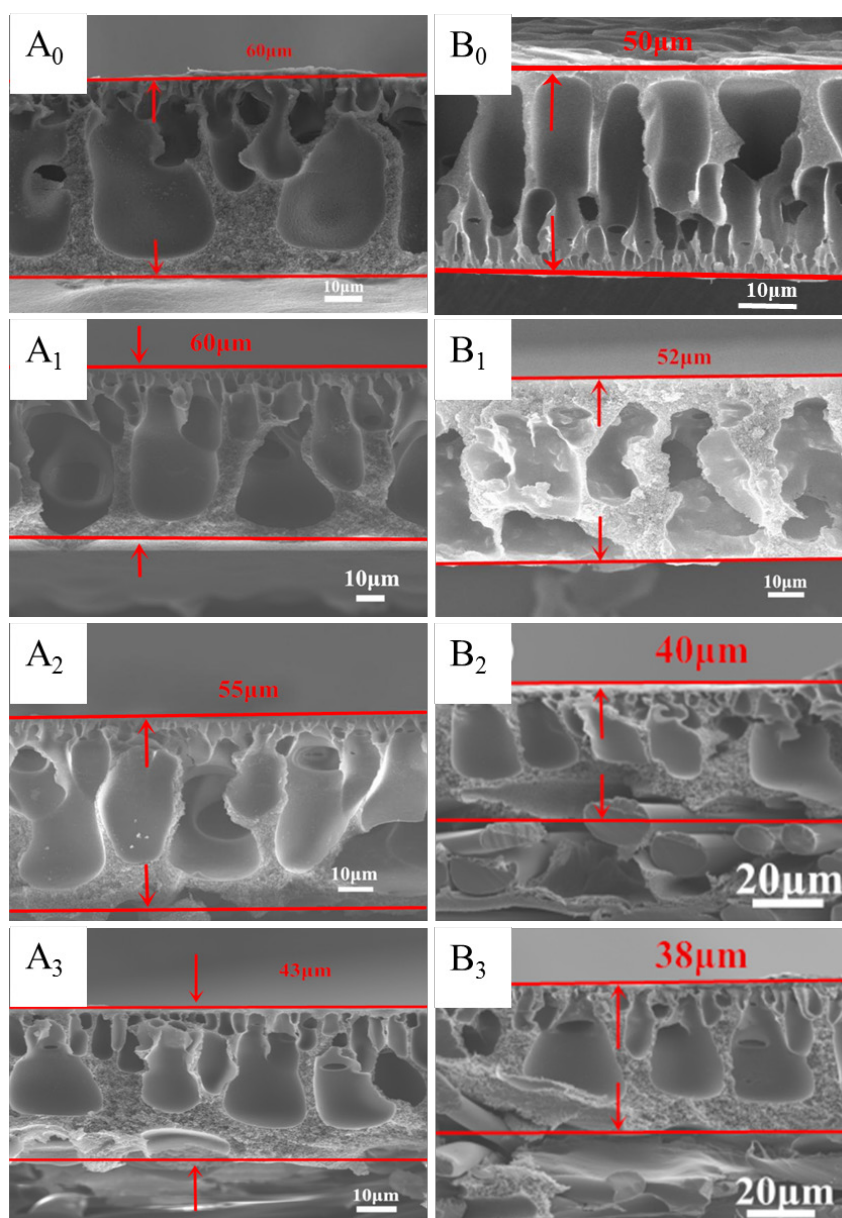
Fig. 5. Comparison of the cross-section morphologies between the PAA membranes (A) and PI membranes (B). The subscript '0' refers to the thermal imidization membrane; '1'-the chemical imidization membrane; '2'-the TER-80 supported membrane; '3'-the UAF-48 supported membrane.

Table 2 shows that both thermally and chemically imidized freestanding PI membranes have much lower overall porosities than the PAA membrane. Although the chemical imidization method cannot avoid the pore collapsing of the PAA membranes, it does alleviate the extent of pore collapsing as compared with the thermal imidization method. Overall porosities of the non-woven supported membranes are about 67~69% which are much higher than those of PI-0 and PI-1. This result proves that the non-woven support can greatly preserve membrane porous structures. In addition, according to Fig. 6, the selective layers' thicknesses only increase from 0.78 μm to 1.04 μm (1.3 times), and 0.61 μm to 0.69 μm (1.1 times), respectively, for the TER-80 and UAF-48 supported membranes. Therefore,

utilization of polyester non-woven supports with chemical imidization is the most efficient method to prevent increment of the PAA selective layer thickness and maintain the overall porosities.

Although the non-woven supports can prevent the formation of wrinkles on the PI membrane surface and reduce the thickening of selective layer, pore sizes of the non-woven fabrics need to be carefully controlled. Fig. 7a$_2$ shows a defect free surface of the TER-80 (with an average pore size of 7.07 μm) supported PI-2. An uneven membrane surface is observed where the dark dots with diameters of 200 nm represent the valley area and the bright parts represent the plateau area. For the UAF-48 non-woven supported PI-3, pores with sizes around 10~20 nm are found on the mem-
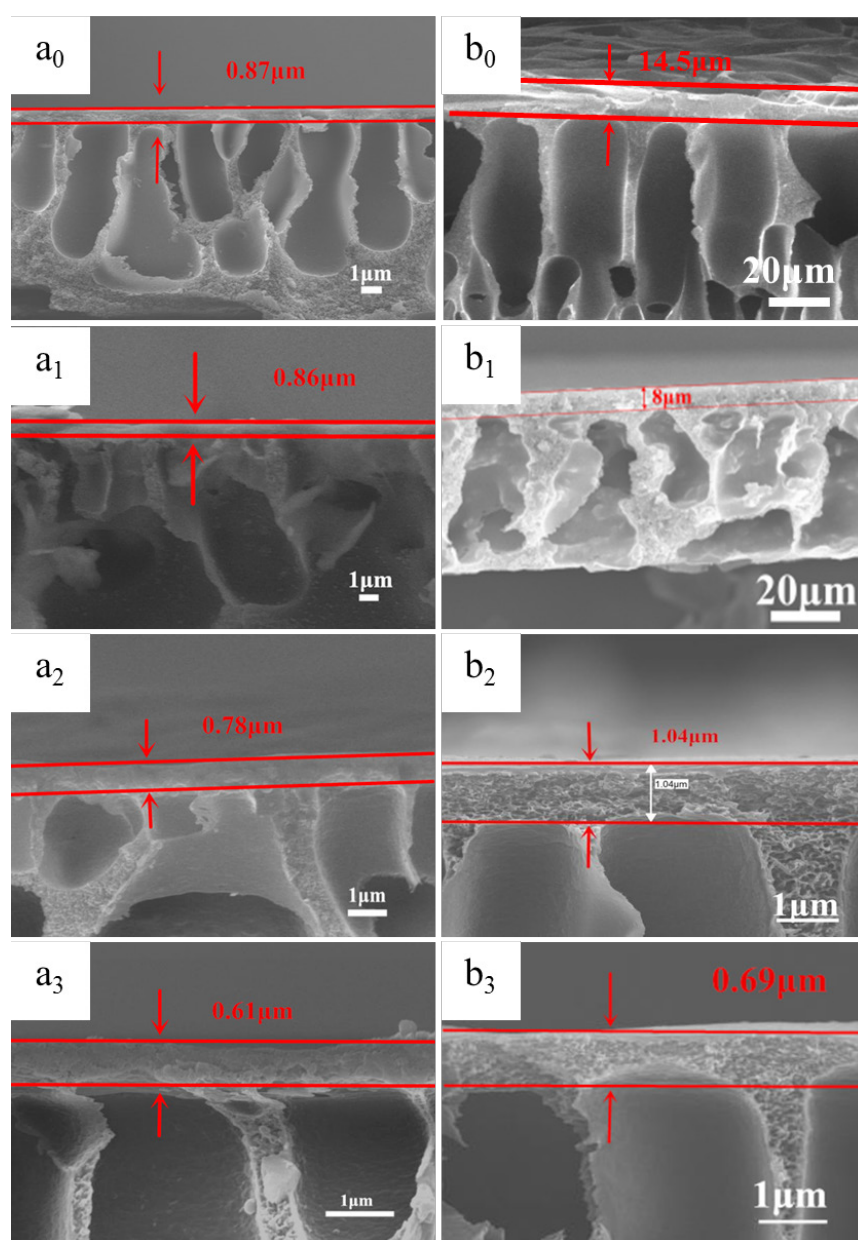
Fig. 6. Changes in the selective layers thicknesses between the PAA membrane (A) and PI membranes (b). The subscript '0' refers to the thermal imidization membrane; '1'-the chemical imidization membrane; '2'-the TER-80 supported membrane; '3'-the UAF-48 supported membrane.

brane surface as shown in Fig 7a$_3$. Formation of defects in PI-3 can be attributed to the infiltration of PAA polymer dope into the UAF-48 non-woven fabric since it has a very large pore size of 25 µm. Fig. 9 shows three-dimensional AFM images of the surfaces of PI-0, PI-1, PI-2 and PI-3. For PI-0 and PI-1, although wrinkles can be observed as shown in Fig. 8b, the membrane surfaces are relatively smooth in a microscopic view. However, as the non-woven fabrics are used as the membrane supports, the surface roughness significantly increases from ~38 nm to 168 nm and 330 nm (root mean square RMS roughness), respectively, for the TER-80 and UAF-48 supported membranes. This result can also be attributed to the infiltration of the polymer dope into the pores of the non-woven supports. As long as the membrane surface is defect free, the higher surface roughness is beneficial for increasing membrane flux since it results in a higher efficient separation area.

3.5. Membrane separation performance

3.5.1. Comparison of the separation performances of PMDA-ODA membranes prepared by different methods

Water permeabilities and rejections to Rose Bengal for PMDA-ODA membranes including PI-0, PI-1, PI-2 and PI-3 were tested at 30°C under 5 bar using both deionized water
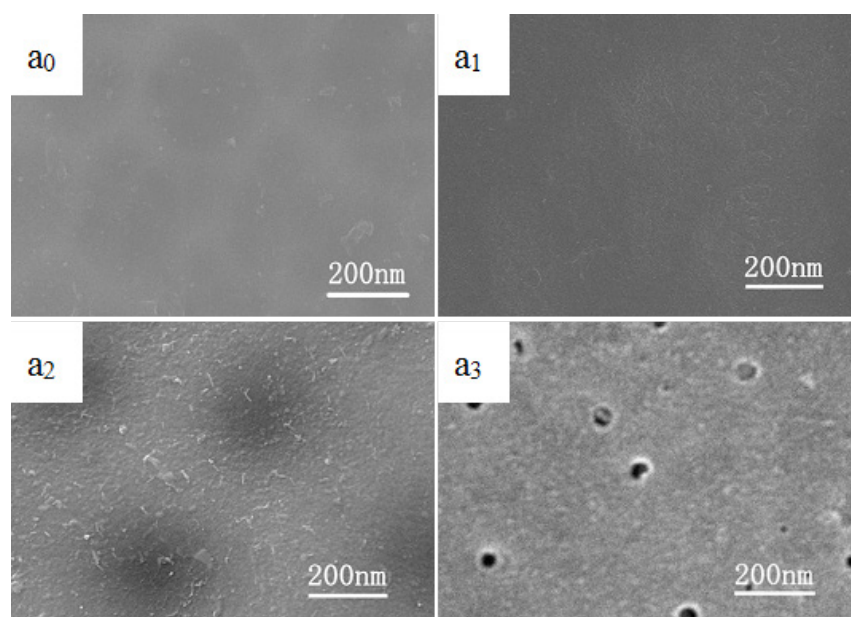
Fig. 7. The surface morphologies of the PMDA-ODA PI membranes: the PI-0 membrane (a_0); the PI-1 membrane (a_1); the PI-2 membrane (a_2); and the PI-3 membrane (a_3).

Table 2
The overall porosities of PMDA-ODA PI membranes.

Membranes	Porosity, %
PAA	80
PI-0	55
PI-1	59
PI-2	67
PI-3	69

and Rose Bengal aqueous solution (100 mg·L^{-1}) as the feeds. As listed in Table 3, both pure water permeability and water permeability of the Rose Bengal aqueous solution decrease in an order of PI-2>PI-1>PI-0. It is in consistent with selective layer thicknesses of the three membranes. Clearly, by (1) replacing thermal imidization with chemical imidization process and (2) adopting the non-woven fabric supports, membrane selective layer thicknesses are greatly reduced which result in the increases in pure water permeabilities from 1.5 L/(m^2·h·bar) to 10.4 L/(m^2·h·bar). Since PI-3 has many defects on the membrane surface, it has the highest water permeability and the lowest rejection to Rose Bengal among all membranes. Since PI-2 exhibits the best separation performance with a high water permeability of 8.7 L/(m^2·h·bar) and 98.0% rejections to Rose Bengal, it is selected for further tests.

3.5.2. Separation performance of the PI-2 membrane at different pressures

Table 4 lists separation properties of PI-2 to 100 mg·L^{-1} Rose Bengal solution at different trans-membrane pressures. As pressure increases from 5 to 20 bar, pure water permeability and water permeability of Rose Bengal solution gradually decrease with a slightly increase in Rose Bengal rejection. This is a typical trend in NF test that can be explained by membrane compression. However, when pressure increases to 25 bar, Rose Bengal rejection drops to 56.6% with a water permeability of 32.4 L/(m^2·h·bar). As the trans-membrane pressure decreases to 5 bar, the Rose Bengal rejection cannot recover to 90%. This indicates that PI-2 membrane is destroyed at 25 bar.

3.5.3. Comparison of separation performances of PI-2 to the thermally imidized PMDA-ODA membrane

NF experiments to different 100 mg·L^{-1} dye solutions were done to evaluate the separation property of PI-2. Table 5 shows that PI-2 has high rejections and water permeabilities to all four dyes. Rejections are in an order of Rhodamine B (94%)<Congo Red (96.3%)<Fast Green FCF (96.8%)<Rose Bengal (97.9%), which follows the same order of dye molecular weights. NF is a process governed by two mechanisms: first, the size exclusion model which is affected by 2 parameters including (i) size of the solute, and (ii) membrane pore size and pore size distributions; and second, the Donnan exclusion principle which is also governed by two factors including (i) solute-membrane charge interactions and (ii) solute electro neutrality [41]. Since PMDA-ODA has a neutral molecular structure and PI-2 shows good rejections (>94%) to dyes with both negative (Rose Bengal, Fast Green FCF, and Congo Red) and positive (Rhodamine B) charges, the Donnan exclusion does not play a major role in dye rejection. Since rejections increase with dye molecular weights, it indicates the steric-hindrance effect or size exclusion dominating the separation processes.

Table 5 also shows that PI-2 has similar dye rejections but 9 to 11 times higher water permeabilities than those of the freestanding PMDA-ODA PI membrane prepared by
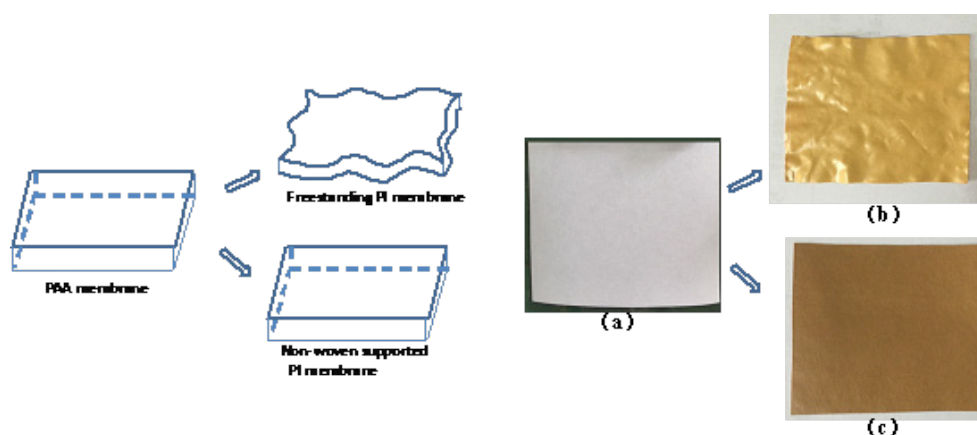
Fig. 8. The illustration and photo images of the PMDA-ODA PAA and PI membranes: (a) PAA membrane; (b) freestanding PI membrane; (c) chemically imidized non-woven supported membrane.
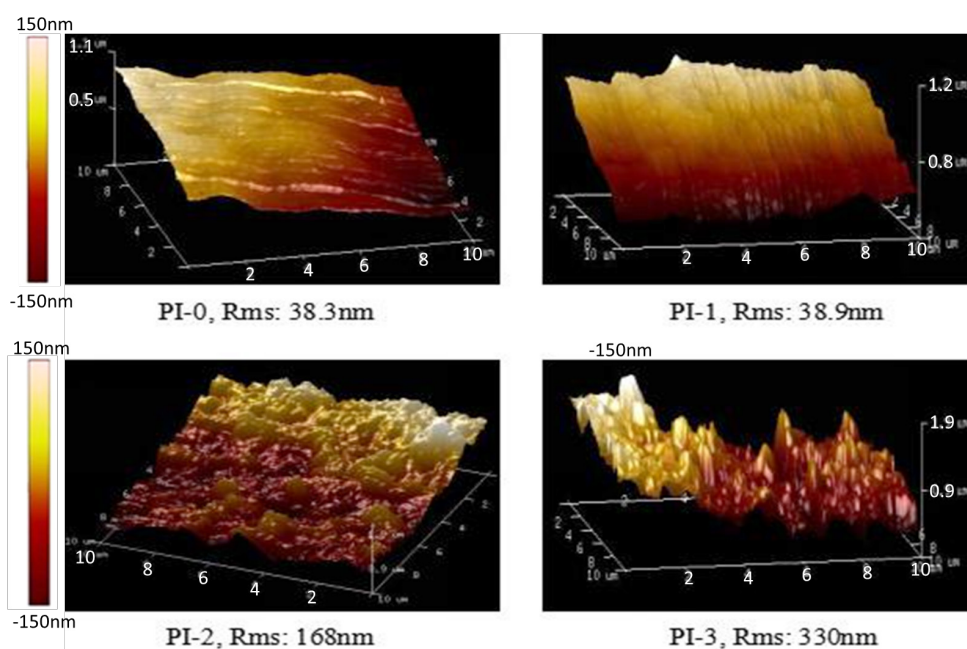
Fig. 9. The AFM images of the surface morphologies of the PI-0, PI-1, PI-2 and PI-3 membranes.

Table 3
The pure water permeabilities and separation performances of PMDA-ODA PI membranes to 100 mg·L⁻¹ Rose Bengal aqueous solution

Membranes	Pure water permeability (L/(m²·h·bar))	Water permeability of Rose Bengal solution (L/(m²·h·bar))	Rose Bengal rejection (%)
PI-0	1.5	0.8	98.5
PI-1	2.9	1.8	98.3
PI-2	10.4	8.7	98.0
PI-3	24.0	16.2	59.4

Table 4
Pure water permeabilities and separation performances of PI-2 membrane to 100 mg·L⁻¹ Rose Bengal aqueous solution at different pressures

Pressure (bar)	Pure water permeability (L/ (m²·h·bar))	Water permeability of Rose Bengal solution (L/(m²·h·bar))	Rose Bengal rejection (%)
5	10.4	8.7	98.0±0.1
10	10.2	8.4	97.9±0.1
15	9.6	8.0	98.1±0.1
20	9.2	7.5	98.3±0.1
25	36.5	32.4	56.6±0.1

Table 5
Permeabilities and rejections to different dye aqueous solutions of PI-2 and PMDA-ODA membranes prepared in our previous work

	Rose Bengal	Fast Green FCF	Congo Red	Rhodamine B
Molecular formula	$C_{20}H_4Cl_4I_4O_5Na_2$	$C_{37}H_{34}N_2O_{10}S_3Na_2$	$C_{32}H_{22}N_6Na_2O_6S_2$	$C_{28}H_{31}ClN_2O_3$
Molecular weight (Da)	1018	809	697	479
Chemical structure				
PI-2 permeability (L/(m²·h·bar))	8.4	9.1	8.4	9.1
PI-2 rejection (%)	97.9	96.7	96.3	94.0
PMDA-ODA membrane [29] permeability (L/(m²·h·bar))	–	1.0	0.9	0.8
PMDA-ODA membrane [29] rejection (%)	–	92	96.2	99.2
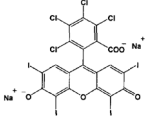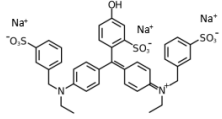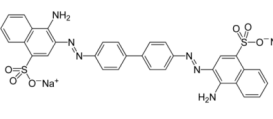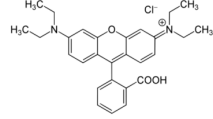
Testing condition: 100 mg·L⁻¹ dye solution, 10 bar.
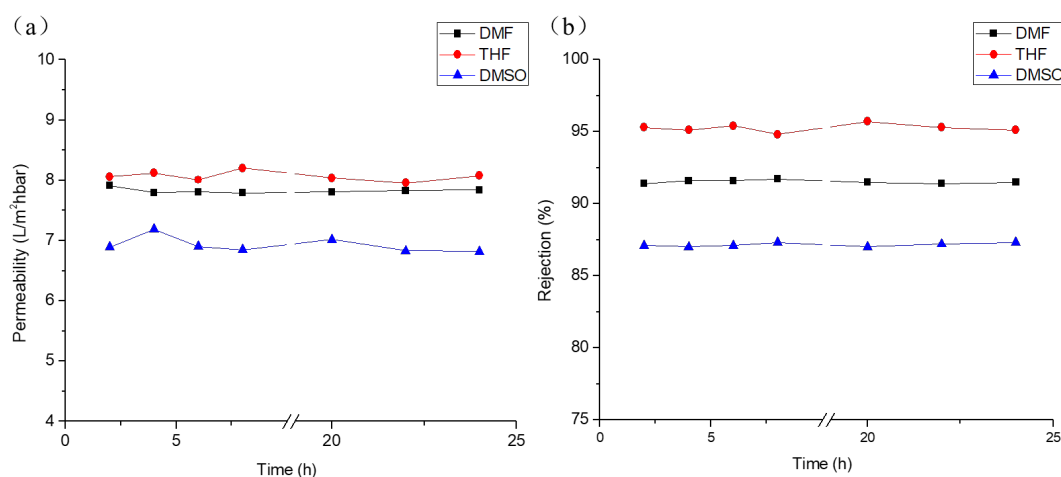
Fig. 10. The (a) permeability and (b) rejection performance of PI-2 in organic dye solutions at room temperature and a transmembrane pressure of 20 bar.

thermal imidization. Clearly, using a polyester non-woven support and chemical imidization can produce PMDA-ODA NF membranes with high solvent permeability without losing rejection properties. Therefore, the PMDA-ODA NF membrane has great potential for separation applications in aqueous systems.

3.5.4. Separation performance of PI-2 in organic solutions

Based on the solubility test results in Table 1, PMDA-ODA is stable in most organic solvents except in NMP, acid and base solutions. To further evaluate the feasibility of PI-2 in aggressive organic solvent systems, 100 mg·L⁻¹ Rose Bengal DMF, THF, DMSO solutions were used as feeds and the NF experiment was continuously running for 24 h to test long term stability of PI-2. Fig. 10 shows that the organic solvent permeabilities are stable during the whole testing period. In addition, rejections of Rose Bengal in DMF, THF,

and DMSO solutions are 91%, 95%, and 87%, respectively. After NF experiments, the PI-2 membrane was rinsed with water and a pure water permeability of 10.4 L/(m²·h·bar) was obtained at a trans-membrane pressure of 5 bar. The similar pure water permeabilities (before and after the organic solution NF experiments) prove that the PMDA-ODA PI membrane maintains its structure during the whole testing period.

4. Conclusion

PMDA-ODA PI has excellent solvent resistance and is an ideal material for fabricating NF membranes in varied solution systems. In this study, we demonstrate that high performance non-woven supported PMDA-ODA NF membrane can be made using a two-step chemical imidization method. Using this protocol, thickness of the membrane

selective layer is only 1.04 µm which is significantly thinner than that of the freestanding thermally imidized membrane (14.5 µm). NF experimental results show that the non-woven supported chemically imidized PMDA-ODA PI membrane has the similar dye rejections as the freestanding thermally imidized membrane but 7 times higher water permeabilities. And the membrane maintains its high performance when separating 100 mg·L^{-1} Rose Bengal organic solutions including DMF, THF, and DMSO, with a permeability of 7.0~8.0 L/(m²·h·bar) and rejections of 87~95% for 24 h operation time. All these results indicate a great potential of the PMDA-ODA NF membrane for industrial applications in both water and organic solvent systems.

Acknowledgements

References

[1] Q. Nan, P. Li, B. Cao, Fabrication of positively charged nanofiltration membrane via the layer-by-layer assembly of graphene oxide and polyethylenimine for desalination, Appl. Surf. Sci., 387 (2016) 521–528.

[2] K. Li, J. Wang, J. Liu, Y. Wei, M. Chen, Advanced treatment of municipal wastewater by nanofiltration: Operational optimization and membrane fouling analysis, J. Environ. Sci., 43 (2016) 106–117.

[3] K. Hendrix, S. Vandoorne, G. Koeckelberghs, I. Vankelecom, OSN membranes for edible oil purification: Introducing free amines in crosslinked PEEK to increase membrane hydrophilicity, Polymer, 55 (2014) 1307–1316.

[4] G. Szekely, M. F.Jimenez-Solomon, P. Marchetti, J.F. Kim, A.G. Livingston, Sustainability assessment of organic solvent nanofiltration: from fabrication to application, Green Chem., 16 (2014) 4440–4473.

[5] J.F. Kim, G. Szekely, M. Schaepertoens, I.B. Valtcheva, M.F. Jimenez-Solomon, A.G. Livingston, In Situ solvent recovery by organic solvent nanofiltration, ACS Sustain. Chem. Eng., 2 (2014) 2371–2379.

[6] J.T. Scarpello, D. Nair, L.M. Freitas dos Santos, L.S. White, A.G. Livingston, The separation of homogeneous organometallic catalysts using solvent resistant nanofiltration, J. Membr. Sci., 203 (2002) 71–85.

[7] L.R. Firman, N.A. Ochoa, J. Marchese, C.L. Pagliero, Deacidification and solvent recovery of soybean oil by nanofiltration membranes, J. Membr. Sci., 431 (2013) 187–196.

[8] D. Darnoko, M. Cheryan, Carotenoids from red palm methyl esters by nanofiltration, J. Amer. Oil Chem. Soc., 83 (2006) 365–370.

[9] K. Ebert, C.F. Petrus, Solvent resistant nanofiltration membranes in edible oil processing, Membr. Technol., 1999 (1999) 5–8.

[10] E.M. Tsui, M. Cheryan, Membrane processing of xanthophylls in ethanol extracts of corn, J. Food Eng., 83 (2007) 590–595.

[11] A. Cassano, W. Cabri, G. Mombelli, F. Peterlongo, L. Giorno, Recovery of bioactive compounds from artichoke brines by nanofiltration, Food Bioprod. Process., 98 (2016) 257–265.

[12] J. Greens, B.D. Witte, B. Vander Bruggen, Removal of API's (active pharmaceutical ingredients) from organic solvents by nanofiltration, Sep. Sci. Technol., 42 (2007) 2435–2449.

[13] F. Weinwurm, A. Drljo, W. Waldmüller, B. Fiala, J. Niedermayer, A. Friedl, Lignin concentration and fractionation from ethanol organosolv liquors by ultra-and nanofiltration, J. Clean. Prod., 136 (2016) 62–71.

[14] W. Puthai, M. Kanezashi, H. Nagasawa, T. Tsuru, Nanofiltration performance of SiO$_2$-ZrO$_2$ membranes in aqueous solutions at high temperatures, Sep. Purif. Technol., 168 (2016) 238–247.

[15] Y. Wang, Y. He, Q. Lai, M. Fan, Review of the progress in preparing nano TiO$_2$: An important environmental engineering material, J. Environ. Sci., 26 (2014) 2139–2177.

[16] D. Hua, T.S. Chung, Polyelectrolyte functionalized lamellar graphene oxide membranes on polypropylene support for organic solvent nanofiltration, Carbon, 122 (2017) 604–613.

[17] Z. Wang, Y.M. Wei, Z.L. Xu, Y. Cao, Z.Q. Dong, X.L. Shi, Preparation, characterization and solvent resistance of γ-Al$_2$O$_3$/α-Al$_2$O$_3$ inorganic hollow fiber nanofiltration membrane, J. Membr. Sci., 503 (2016) 69–80.

[18]. T. Tsuru, T. Nakasuji, M. Oka, M. Kanezashi, T. Yoshioka, Preparation of hydrophobic nanoporous methylated SiO$_2$ membranes and application to nanofiltration of hexane solutions, J. Membr. Sci., 384 (2011) 149–156.

[19] R. Gracia, S. Cortes, J. Sarasa, P. Ormad, J.L. Ovelleiro, TiO$_2$-catalysed ozonation of raw Ebroriver water, Water Res., 34 (2000) 1525–1532.

[20] R. Boussahel, A. Montielb, M. Baudu, Effects of organic and inorganic matter on pesticide rejection by nanofiltration, Desalination, 145 (2002) 109–114.

[21] B.V.D. Vander Bruggen, J. Geens, C. Vandecasteele, Fluxes and rejections for nanofiltration with solvent stable polymeric membranes in water, ethanol and n-hexane, Chem. Eng. Sci., 57 (2002) 2511–2518.

[22] H. Tham, K.Y. Wang, D. Hua, S. Japip, T.S. Chung, From ultrafiltration to nanofiltration: Hydrazine cross-linked polyacrylonitrile hollow fiber membranes for organic solvent nanofiltration, J. Membr. Sci., 542 (2017) 289–299.

[23] N.W. Oh, J. Jegal, K.H. Lee, Preparation and characterization of nanofiltration composite membranes using polyacrylonitrile (PAN). I. Preparation and modification of PAN supports, J. Appl. Polym. Sci., 80 (2001) 1854–1862.

[24] S. Aerts, H. Weyten, A. Buekenhoudt, L.E. Gevers, I.F. Vankelecom, P.A. Jacobs, Recycling of the homogeneous Co-Jacobsen catalyst through solvent-resistant nanofiltration (SRNF), Chem. Commun., 6 (2004) 710–711.

[25] Y. Wang, L.Y. Jiang, T. Matsuura, T.S. Chung, S.H. Goh, Investigation of the fundamental differences between polyamide-imide (PAI) and polyetherimide (PEI) membranes for isopropanol dehydration via pervaporation, J. Membr. Sci., 318 (2008) 217–226.

[26] I.B. Valtcheva, P. Marchetti, A.G. Livingston, Crosslinked polybenzimidazole membranes for organic solvent nanofiltration (OSN): Analysis of crosslinking reaction mechanism and effects of reaction parameters, J. Membr. Sci., 493 (2015) 568–579.

[27] S. Tsarkov, V. Khotimskiy, P.M. Budd, V. Volkov, J. Kukushkina, A. Volkov, Solvent nanofiltration through high permeability glassy polymers: Effect of polymer and solute nature, J. Membr. Sci., 423–424 (2012) 65–72.

[28] A. Gupta, N.B. Bowden, Separation of cis-Fatty acids from saturated and trans-Fatty acids by nanoporous polyicyclopentadiene membranes, ACS Appl. Mater. Interf., 5 (2013) 924–933.

[29] P. Vandezande, X.F. Li, L.E.M. Gevers, I.F.J. Vankelecom, High throughput study of phase inversion parameters for polyimide-based OSN membranes, J. Membr. Sci., 330 (2009) 307–318.

[30] A.F. Ismail, L.P. Yean, Review on the development of defect-free and ultrathin-skinned asymmetric membranes for gas separation through manipulation of phase inversion and rheological factors, J. Appl. Polym. Sci., 88 (2003) 442–451.

[31] M. Farahani, D. Hua, T.S. Chung, Cross-linked mixed matrix membranes consisting of carboxyl-funcitnalized multi-walled carbon nanotubes and P84 polyimide for organic solvent nanofiltration (OSN), Sep. Purif. Tech., 186 (2017) 243–254.

[32] A.A. Tashvigh, L. Luo, T.S. Chung, M. Weber, C. Maletzko, A novel ionically cross-linked sulfonated polyphenylsulfone (sPPSU) membrane for organic solvent nanofiltration (OSN), J. Membr. Sci., 545 (2018) 221–228.

[33] L.B. Nohara, M.L. Costa, M.A. Alves, M.F.K. Takahashi, E.L. Nohara, M.C. Rezende, Processing of high performance composites based on PEEK by aqueous suspension prepregging, Mater. Res., 13 (2010) 245–252.

[34] B. Fang, K. Pan, Q.H. Meng, B. Cao, Preparation and properties of polyimide solvent-resistant nanofiltration membrane obtained by a two-step method, Polym. Int., 61 (2012) 111–117.

[35] J.Q. Wang, K.Y. Song, B. Cao, L. Li, K. Pan, The influence of polyamic acid molecular weight on the membrane structure and performance of polyimide solvent-resistant nanofiltration, J. Chem. Technol. Biotechnol., 91 (2016) 777–785.

[36] M. Kotera, T. Noshino, K. Nakamae, Imidization processes of aromatic polyimide by temperature modulated DSC, Polymer, 41 (2000) 3615–3619.

[37] C. Ba, Economy, J. Preparation of PMDA/ODA polyimide membrane for use as substrate in a thermally stable composite reverse osmosis membrane, J. Membr. Sci., 363 (2010) 140–148.

[38] C. Ma, W.J. Koros, Effects of hydrocarbon and water impurities on CO_2/CH_4 separation performance of ester-crosslinked hollow fiber membranes, J. Membr. Sci., 451 (2014) 1–9.

[39] Y. Li, B. Cao, P. Li, Fabrication of PMDA-ODA hollow fibers with regular cross-Section morphologies and study on the formation mechanism, J. Membr. Sci., 544 (2017) 1–11.

[40] J.D. Wind, D.R. Paul, W.J. Koros, Natural gas permeation in polyimide membranes, J. Membr. Sci., 228 (2004) 227–236.

[41] X. Wang, X. Ju, T.Z. Jia, Q.C. Xia, J.L. Guo, C. Wang, Z. Cui, Y. Wang, W. Xing, S.P. Sun, New surface cross-linking method to fabricate positively charged nanofiltration membranes for dye removal, J. Chem. Tech. Biotech., (2018) DOI: 10.1002/jctb.5571.